Lawrence Berkeley National Laboratory

Title
Pore connectivity effects on solute transport in rocks

Permalink
https://escholarship.org/uc/item/69b8w00n

Authors
Hu, Qinhong
Ewing, Robert P.

Publication Date
2001-11-30

Pore Connectivity Effects on Solute Transport in Rocks

Qinhong Hu, Lawrence Berkeley National Laboratory
Robert P. Ewing, Iowa State University

Abstract

Retardation of nuclear contaminants in rock matrices can lead to long retention times, allowing substantial radionuclide decay prior to eventual release. Imbibition and diffusion into the rock matrix can move contaminants away from an active fracture, thereby contributing to their retardation. However, diffusive transport in some rocks may behave anomalously because of their sparsely connected porespace, in contrast to diffusion in rocks with denser pore connections. We examined imbibition of weakly sorbing tracers into welded tuff and Indiana sandstone, and water imbibition into metagraywacke and Berea sandstone. Tuff samples were initially equilibrated to 12% and 76% water (v/v) within controlled humidity chambers, while the other rocks were air-dried. For imbibition, one face was exposed to water, with or without tracer, and uptake was measured over time. Following imbibition, tracer concentration measurements were made at fine (1 mm) increments. Three anomalous results were observed: (1) Indiana sandstone and metagraywacke showed mass of imbibed water scaling as $time^{0.26}$, while tuff and Berea sandstone showed the more classical scaling with $time^{0.5}$; (2) tracer movement into dry (2% initial saturation) Indiana sandstone showed a dispersion pattern similar to that expected during tracer movement into moist (76% initial saturation) tuff; and (3) tracer concentrations at the inlet face of the tuff sample were approximately twice those deeper inside the sample. The experiment was then modeled using random walk methods on a 3-D lattice with different values of pore coordination. Network model simulations that used a pore coordination of 1.49 for Indiana sandstone and 1.56 for metagraywacke showed similar temporal scaling, a result of their porespace being close to the percolation threshold. Tracer concentration profiles in Indiana sandstone and tuff were closely matched by simulations that used pore coordinations of 1.49 and 1.68, respectively, because of how low connectivity alters the accessible porosity in the vicinity of the inlet face. The study supports pore connectivity as a coherent explanation for the observed anomalies and demonstrates the utility of pore-scale modeling in elucidating mechanisms critical to radionuclide retardation in geological repositories.

Introduction

Conservative assessment of the long-term fate of radioactive waste assumes that some leakage from the waste packages will occur. An appropriate design strategy is to assure that migration of leaking materials is slow enough that considerable radioactive decay will occur during the leakage and migration phase. To this end, waste may be confined in rock repositories, because diffusion into and through rock is relatively slow, thus assuring the needed time. Such a strategy is used in the potential high-level nuclear waste repository at Yucca Mountain, NV, USA.

The picture at Yucca Mountain, and in rocks generally, is complicated by the presence of fractures. These fractures can function as high-velocity flow pathways, with solutes being both dispersed and retarded via diffusive exchange between the fracture and the rock matrix. If the matrix is even slightly below saturation, imbibition from active fractures will augment the diffusive movement of solutes from fracture to matrix. Accurate assessment of rock matrix imbibition and diffusion is therefore a key issue in evaluating an unsaturated repository site.

It is well established that diffusion and dispersion are often scale-dependent (Tyler and Wheatcraft, 1988; Berkowitz and Scher, 1998). Most explanations of this phenomenon invoke increasing heterogeneity at increasing scales, but such heterogeneity is not always observed. A different explanation was recently advanced by Ewing and Horton (2002a,b), who showed through pore-scale diffusion modeling that low connectivity at the pore scale could lead to diffusivity decreasing with increasing time and/or distance. In essence, low connectivity can cause increasing heterogeneity of flowpaths at increasing scales, even though the connectivity itself, as well as macroscopic properties such as porosity, may be spatially homogeneous.

Imbibition of water from active fractures into an unsaturated matrix can be a critical contributor to solute exchange between fracture and matrix. Furthermore, imbibition is mathematically a diffusive process, so its behavior should be related to diffusive behavior. Hu et al. (2002 and unpublished results) examined imbibition of tracer-laced water into rocks, and observed three apparently anomalous results: first, while the imbibition front is generally expected to advance in proportion to the square root of time (Philip, 1957), in some rocks an advance approximately proportional to the fourth root of time is observed. Second, while a tracer concentration profile is expected to resemble the saturation profile during imbibition into initially dry media but show greater dispersion during imbibition into wet media, high apparent dispersion was observed during imbibition into initially air-dry Indiana sandstone. And third, an apparently anomalous increase in porosity was observed at the inlet face during imbibition into welded tuff, even

though this face was prepared from the inside of a solid sample rather than from a weathered fracture face.

The objective of this research was to investigate pore connectivity as a potential cause of these three anomalous observations, through comparison of laboratory imbibition experiments with pore-scale imbibition simulations.

Methods:

Rocks used were welded tuff, Berea sandstone, Indiana sandstone, and metagraywacke. Rock properties are summarized in Table 1. The imbibition protocols are described by Hu et al. (2001). Briefly, cylindrical rock cores (2 cm length, 5 cm diameter) with epoxy-coated sides and exposed top and bottom faces are equilibrated in controlled humidity chambers to the desired water contents, approximately 2% (air-dry), 12.5%, and 76% saturation. They are then suspended, from an analytical balance, in a chamber with a water pan, such that the bottom face of the core contacts the free water surface. Balance readings are initially recorded at 3 s intervals, with time intervals increasing over the duration of the experiment. Imbibition is calculated from the cumulative change in suspended mass over time, with corrections for buoyancy resulting from changes in the water level caused by both imbibition and evaporative losses from the chamber (Hu et al., 2001). For welded tuff and Indiana sandstone, the procedure was modified by the addition of multiple tracers (bromide [nonsorbing], Sulpho-Rhodamine B [sorption coefficient 0.09 mL/g], and FD&C Blue #1 [sorption coefficient 0.06 mL/g]) to the water. Upon completion of the imbibition phase of the experiment, small holes were drilled into the cores from both the inlet and air-exit faces, with rock powder sampled at 1 mm depth intervals. Tracer concentrations in the rock powder were measured using an ion-specific electrode (bromide), a fluorometer (Sulpho-Rhodamine B), or a UV/Vis spectrophotometer (FD&C Blue #1). Further details concerning rock drilling and analysis of tuff can be found in Hu et al. (2002).

Table 1. Properties of the rocks used.

Rock	% Porosity	Permeability, m^2	% Initial Saturation	Tracers	Source
Berea Sandstone	22.8	$9.1 * 10^{-13}$	Air-dry*	None	Berea Quarry, OH, USA
Indiana Sandstone	17.6	$1.8 * 10^{-13}$	Air-dry*	Bromide FD&C Blue #1 Sulpho-Rhodamine B	Gas Storage Formation, IN, USA
Welded Tuff	9.25	$5.0 * 10^{-19}$	12.5 76.0	Bromide FD&C Blue #1 Sulpho-Rhodamine B	Potential high-level nuclear waste repository, Yucca Mtn., NV, USA (Hu et al., 2002)
Meta-graywacke	3.85	$1.2 * 10^{-17}$	Air-dry*	None	The Geysers, CA, USA (Persoff and Hulen, 2001)

*: Air-dry was assumed to be 2% saturation

The pore-scale modeling conceptualizes the rock matrix as an assemblage of pore bodies connected by pore throats. Rocks with well-interconnected porespaces, such as non-cemented sandstones, have coordination (mean number of pore bodies to which each body is connected) in the range of $z = 4$–8 (Lin and Cohen, 1982; Yanuka et al., 1984). Note that the coordination number given applies to the entire network: even at the percolation threshold, pores that are part of the "infinite cluster" have on average a coordination number no less than 2.0 (Ewing and Horton, 2002a). We used a cubic lattice ($z = 6$) and pruned connections at random to arrive at the desired coordination. Because our interest was in exploring the effects of pore connectivity, in this study we ignore issues such as pore size. Related stochastic process models that focus on medium properties other than the pore size distribution have been described by Flury and Flühler (1995), Trantham and Durnford (1999), and Ewing and Horton (2002a,b).

The stochastic process model anti-DLA (anti-Diffusion-Limited Aggregation; also called internal DLA; see Paterson, 1984; Meakin and Deutch, 1986) has been identified as an analog for stable displacement during imbibition (Lenormand, 1990). The choice of anti-DLA as the underlying imbibition model in this research is justified by the observations that imbibition upward is gravity-stabilized, the viscosity ratio is positive, and imbibition into low aspect ratio media generally shows a stable front at almost any capillary number (Lenormand, 1990). In anti-DLA,

a random walker starts at a source location within phase A and diffuses until it reaches a phase B point, whereupon it stops, converting that point to A. As applied to our physical situation, free water at the inlet face of the core is the source point, and a random walker diffuses through water-filled pores into the core. Upon reaching a pore that is not occupied by water, it fills the pore, and a new walker is initiated. The anti-DLA model is diffusion based, so (for example) scaling of cumulative imbibed mass with the square root of time is an expected macroscopic behavior, although it is not explicitly programmed to occur.

In this model, random walkers cannot move across connections that have been pruned. Antecedent saturation is included simply by marking some proportion of the matrix pores as water-filled at the outset. Progress of the imbibition process is recorded whenever 100 particles have imbibed, and a saturation profile is written when the wetting front first touches the far end of the lattice. Modeling the placement of retarding tracers takes into account both the retardation factor and the antecedent saturation. Specifically, tracers were emplaced as the average of (1) the final position of a water molecule divided by the retardation factor, weighted by antecedent unsaturation, and (2) the (total time/retardation^2)th position of a diffusing water molecule, weighted by antecedent saturation. We used a 100 x 50 x 50 site lattice, emplacing 10,000 tracer molecules per realization and averaging results over five realizations.

Results and Discussion

1. Temporal Behavior of Imbibition

The absolute rates of imbibition are functions of the pore size distribution and porosity, and do not concern us here. Imbibition into Berea sandstone and welded tuff scaled with the square root of time (Figure 1), as is generally expected (Philip, 1957). However, imbibition into metagraywacke (early time only) and Indiana sandstone scaled approximately with time$^{0.26}$. This scaling result matches predictions of percolation theory (Stauffer and Aharony, 1992) for 3-D diffusion at the percolation threshold, the coordination at which a sparsely connected porespace is only just connected.
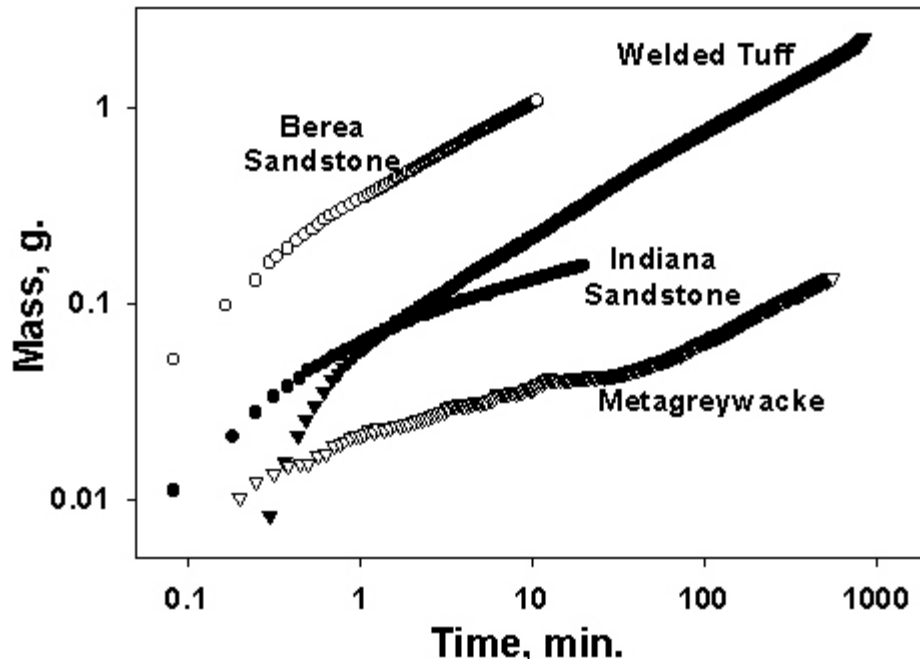
Figure 1. Experimental results showing cumulative imbibition into Berea sandstone, Indiana sandstone, welded tuff, and metagraywacke.

Simulations of imbibition match the experimental data well, showing an initially steep period (rapid wetting of the inlet face) followed by a fairly straight section (Figure 2). The slope of the straight section is 0.5 at high ($z > 1.68$) connectivities. Progressively lower pore coordination results in a lower imbibition rate, and eventually a change in the temporal scaling. Notice that at low but noncritical values of connectivity ($z = 1.56$), the slope soon stabilizes at a slope of 0.26, then eventually reverts to 0.5. Likewise, the imbibition plot of metagraywacke (Fig. 1) suggests that around 50 minutes, it undergoes a gradual transition from short term, 0.26-slope behavior to longer-term, 0.5-slope behavior. A similar transition, from 0.26-slope at early times to 0.50-slope at later times, was observed by Ewing and Horton (2002a) for diffusion in lattices slightly above criticality. Pore connectivity therefore provides a simple, unified explanation for the observed anomaly.
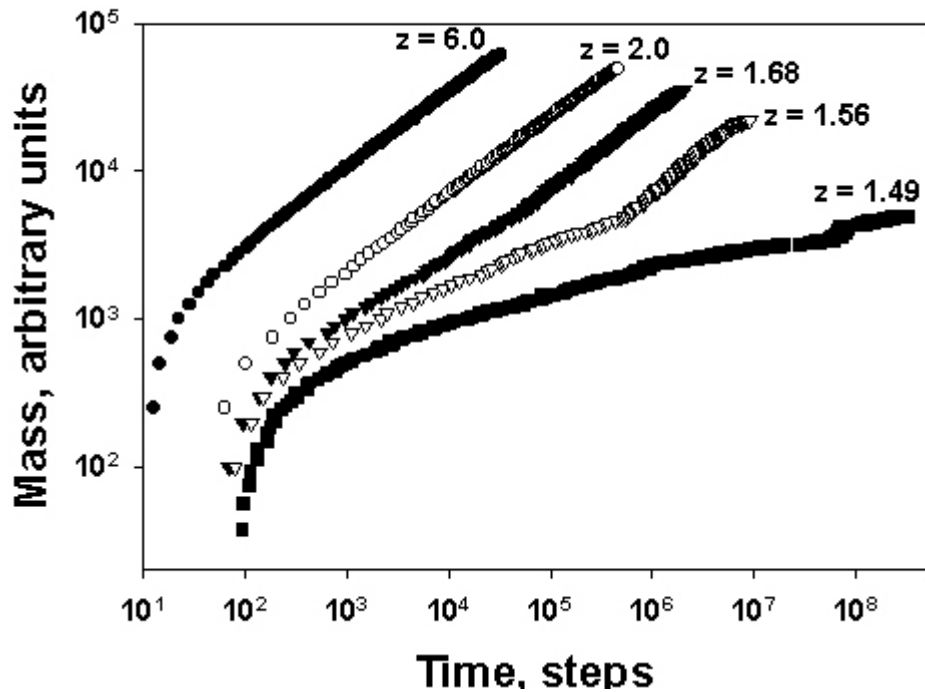
Figure 2. Simulation of cumulative imbibition over a range of pore coordinations.

2. Tracer Dispersion with Initial Saturation

During imbibition into a dry medium, a solute concentration profile typically will resemble the saturation profile, with retardation changing the position but not the shape of the profile. In contrast, during imbibition into a moist medium, solutes will disperse by mixing with "old" water, and so a less sharp profile would generally be observed. These trends are illustrated for the case of dye imbibition into welded tuff, where a more dispersed distribution is observed at 76% than at 12.5% initial saturation (Figure 3). However, against usual expectations, tracer concentration profiles for dye imbibition into air-dry Indiana sandstone show the high-dispersion pattern seen with imbibition into moist (76% initial saturation) tuff.

Simulations using a pore coordination of $z = 1.49$ (at the percolation threshold) for "Indiana sandstone" and $z = 1.68$ for "welded tuff" (Figure 4) show a pattern similar to those observed experimentally (Figure 3). The tracer concentration profile following simulated imbibition into the dry "tuff" is similar to the wetting front after adjustment for retardation (not shown), while that following simulated imbibition into the moister "tuff" shows more retardation and dispersion. This indicates that the particle emplacement algorithm gives the correct behavior with

respect to antecedent saturation. Of greater interest is that the tracer profile in the simulated Indiana sandstone also matches the experimental data fairly well. The explanation for this tracer profile in the "Indiana sandstone" lies not in dispersion mechanisms, but in the spatial distribution of accessible porosity in a low-coordination porous medium.
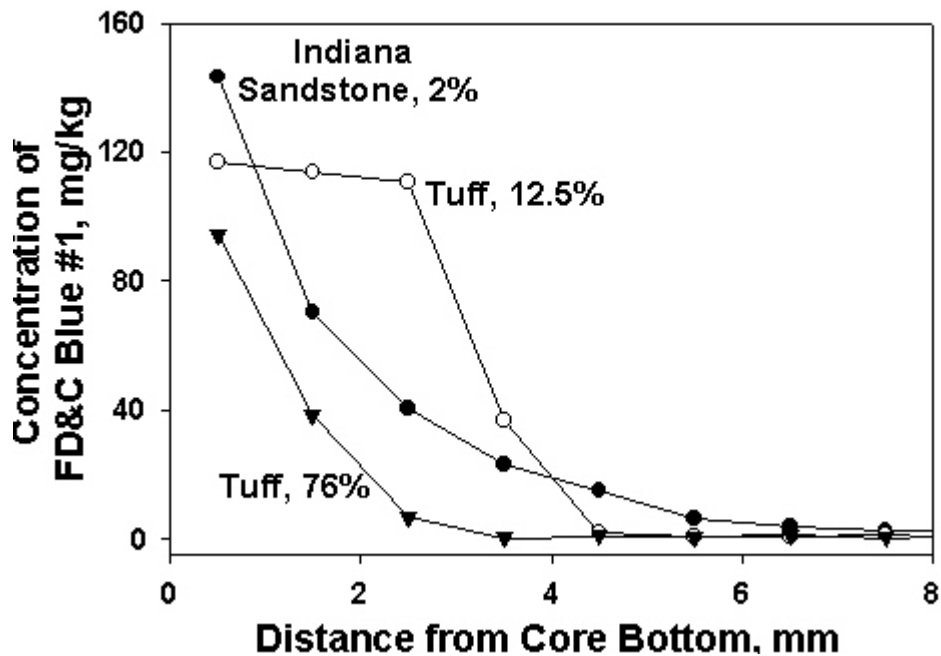

Figure 3. Concentration profiles of a weakly sorbing dye following imbibition into welded tuff (12.55 and 76% initial saturation) and air-dry Indiana sandstone. Data for Bromide and Sulpho-Rhodamine B (not shown) exhibit similar behavior.

Recall that the Indiana sandstone core showed an imbibition plot slope of 0.26, in contrast to the more classical 0.5; an explanation can therefore be based on Indiana sandstone being at the percolation threshold. Near and at the percolation threshold, the porosity accessible from one end varies as a function of distance from the exposed face (Ewing and Horton, 2002b). This phenomenon is illustrated by the dotted lines in Figure 5, showing accessible porosity from 5 realizations on a cubic lattice at two different coordinations, scaled to match the Indiana sandstone bromide curve. The agreement between the two curves supports low pore connectivity as a reasonable explanation. In other words, the tracer profile in the Indiana sandstone is caused not by dispersion, but rather by the accessible porosity.
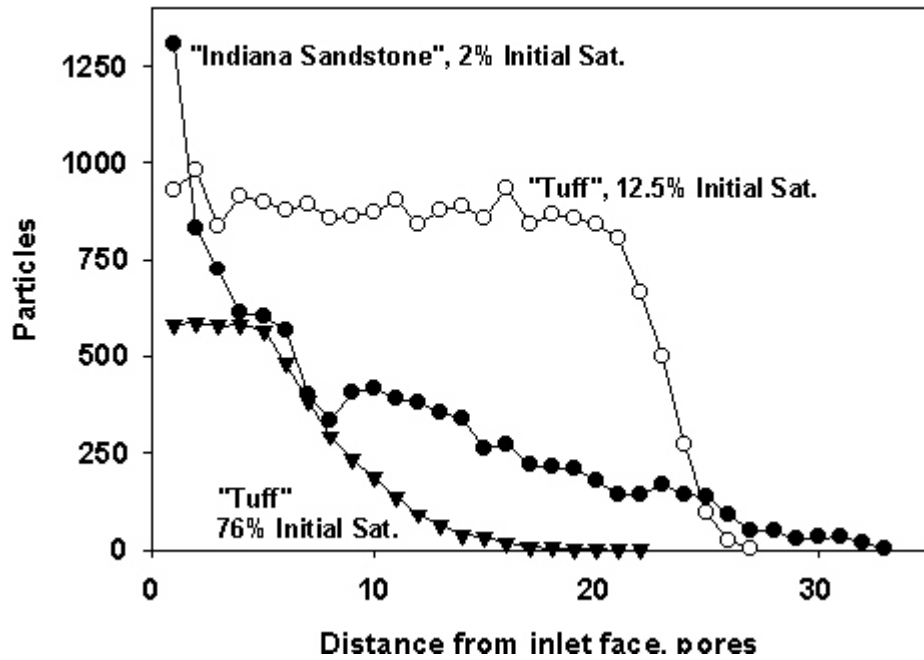
Figure 4. Simulated concentration profiles of dyes following imbibition.
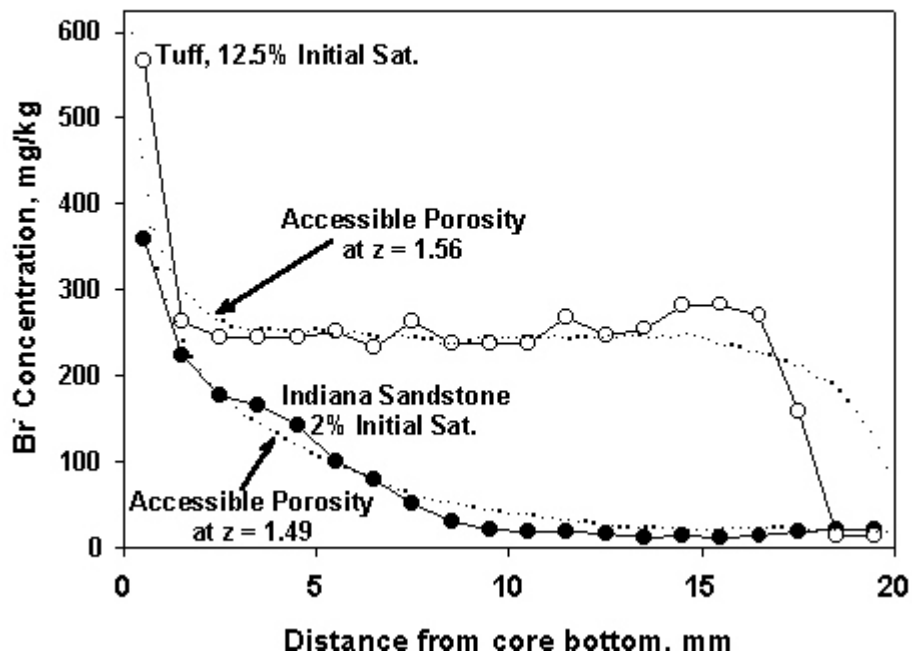

Figure 5. Concentration profiles of bromide following imbibition into welded tuff (12.5% initial

saturation) and air-dry Indiana sandstone. Dotted lines show theoretical predictions of accessible porosity (normalized to the bromide concentrations) at coordination numbers of 1.49 (for Indiana sandstone) and 1.56 (for tuff).

3. Tracer Concentrations at the Fracture Face

In several of the welded tuff cores with initial saturation of 12.5%, bromide concentration in the millimeter closest to the inlet end was approximately twice the concentration through the rest of the core (Figure 5). This might initially have been thought a measurement error had it not been observed in multiple cores, with proportions of edge to plateau concentration ranging from 1.45 to 2.17. Again, pore connectivity considerations can explain the disparity. As with the tracer concentration profile in Indiana sandstone, it appears that the apparently anomalous reading at the inlet end is an artifact of differences in accessible porosity with position. The difference between coordination numbers of 1.56 and 1.49 appears quite small, but the difference in the corresponding accessible porosity profiles is dramatic (Fig. 5). Again, pore connectivity provided a simple and coherent explanation for the observed anomalies.

Conclusions

We examined imbibition and/or tracer concentration profiles in four rocks, and simulated several of the tracer imbibition experiments to more closely examine results that appeared anomalous. Pore connectivity near or at the percolation threshold appeared to be the root cause in all cases, explaining the anomalous temporal scaling of cumulative imbibition in Indiana sandstone and metagraywacke, the apparent dispersion during imbibition into air-dry Indiana sandstone, and the high tracer concentrations at the inlet edge of welded tuff. The anti-DLA-based imbibition model matched experimental results quite well, giving us a useful new simulation tool and helping to evaluate a simple and consistent explanation for the observed anomalies.

References:

Berkowitz, B. and H. Scher, Theory of anomalous chemical transport in fracture networks, Phys. Rev. E 57:5858-5869, 1998.

Ewing, R.P. and R. Horton, Diffusion in sparsely connected porespaces. I. Time-dependent processes, Water Resour. Res. (submitted), 2002a.

Ewing, R.P. and R. Horton, Diffusion in sparsely connected porespaces. II. Steady-state distance-dependent processes, Water Resour. Res. (submitted), 2002b.

Flury, M. and H. Flühler, Modeling solute leaching in soils by diffusion-limited aggregation: Basic concepts and application to conservative solutes, Water Resour. Res. 31:2443-2452, 1995.

Hu, M.Q., P. Persoff, and J.S.Y. Wang, Laboratory measurement of water imbibition into low-permeability welded tuff, J. Hydrol. 242:64-78, 2001.

Hu, M.Q., T.J. Kneafsey, R.C. Trautz, and J.S.Y. Wang, Tracer penetration into welded tuff matrix from flowing fractures, Vadose Zone J. (submitted), 2002.

Lenormand, R., Liquids in porous media, J. Phys: Condensed Matter 2, SA79-88, 1990.

Lin, C. and M.H. Cohen, Quantitative methods for microgeometric modeling, J. Appl. Phys. 53:4152-4165, 1982.

Meakin, P. and J.M. Deutch, The formation of surfaces by diffusion limited annihilation, J. Chem. Phys. 85:2320-2325, 1986.

Paterson, L., Diffusion-limited aggregation and two-fluid displacements in porous media, Phys. Rev. Lett. 52:1621-1624, 1984.

Persoff, P. and J.B. Hulen, Hydrologic characterization of reservoir metagraywacke from shallow and deep levels of The Geysers vapor-dominated geothermal system, California, USA, Geothermics 30:169-192, 2001.

Philip, J.R., The theory of infiltration: 4. Sorptivity and algebraic infiltration equations, Soil Sci. 84:257-265, 1957.

Stauffer, D. and A. Aharony, *Introduction to Percolation Theory* (2nd Ed.), Taylor and Francis, London, 1992.

Trantham, H. and D. Durnford, Stochastic aggregation model (SAM) for DNAPL-water displacement in porous media, J. Contam. Hydrol. 36:377-400, 1999.

Wheatcraft, S.W. and S.W. Tyler, An explanation of scale-dependent dispersivity in heterogeneous aquifers using concepts of fractal geometry, Water Resour. Res. 24:566-578, 1988.

Yanuka, M, F.A.L. Dullien, and D.E. Elrick, Serial sectioning digitization of porous media for two- and three-dimensional analysis and reconstruction, J. Micros. 135:159-168, 1984.